Some Preparative Methods and Physical Characteristics Of Uranium Dioxide Powders

J. C. CLAYTON and SEYMOUR ARONSON
Bettis Atomic Power Laboratory, Westinghouse Electric Corp., Pittsburgh 30, Pa.

URANIUM dioxide has become of considerable importance as a nuclear fuel in the field of atomic power. Published data on the surface area, density, porosity, crystallite size, microstructure, and sinterability of this compound show wide variations (*1, 3, 5, 17-19, 23*). Considerable evidence shows that characteristics of powders, such as uranium oxides, are determined largely by their preparative history. It was ascertained that the density and surface area of UO_2, uranium dioxide, preparations depend upon the density and surface area of the substance from which the UO_2 was prepared (*1, 5*). The present study was undertaken to find the relationships between the method of preparation of UO_2 and its physical properties. Information was sought regarding the effects of chemical processes on microstructure, density, surface area, porosity, crystallite size, and particle size distribution.

EXPERIMENTAL METHODS

Preparation of UO_2 Powder. UO_2 was made by several oxidation and reduction methods, including hydrogen reduction of the higher uranium oxides (UO_3, $UO_2 \cdot 2H_2O$, $UO_3 \cdot H_2O$, and U_3O_8) at temperatures ranging from 500° to 1700° C. as well as by steam and air oxidation of uranium hydride and uranium metal. The methods are summarized in Table I. These UO_2 powders were nonpyrophoric in all cases. UO_2 was also prepared from precipitated U(VI) salts. Ammonium diuranate, $(NH_4)_2U_2O_7$, was precipitated from hot (90° C.), 0.5*M* uranyl nitrate solutions by the addition of ammonium hydroxide, gaseous ammonia, urea, and ammonium carbonate. The crystals produced by reaction with 1:1 ammonium hydroxide showed a wide range of irregular shapes and sizes. The pH of precipitation was 8. Uniform spherical particles of ammonium diuranate were obtained by precipitation with a 20% ammonium carbonate solution at a pH of 3. Very fine, minute ammonium diuranate particles were obtained by bubbling gaseous ammonia through a fritted glass disk dispersion tube into a uranyl nitrate solution. Solutions containing 0.1*M* uranyl nitrate and 0.7*M* urea were boiled for 2 hours to hydrolyze the urea. The decomposition of urea resulted in homogeneous generation of ammonium hydroxide in solution. The pH of precipitation was 6.5. Uranium peroxide, $UO_4 \cdot 2H_2O$, was precipitated from hot (90° C.) 0.5*M* uranyl nitrate solution by the slow addition of 10% hydrogen peroxide. The pH of precipitation was 1.5. Uranyl oxalate, $UO_2(C_2O_4)_2 \cdot H_2O$, was precipitated from hot (90° C.) 0.5*M* uranyl nitrate solution by the slow addition of 10% oxalic acid at a pH of 2. All the precipitates were digested for 1 hour at 90° C.,

Table I. UO_2 Preparation Methods

Method of Preparation	Reaction Conditions		O/U Ratio	Color
	Temp., ° C.	Time, hr.		
High pressure (2200 p.s.i.g.) steam oxidation of uranium	343	6–72	1.85–1.99	Black
Controlled low pressure (3.5–7.5 p.s.i.g.) steam oxidation of uranium	150–250	8–16	2.01–2.05	Black
Uncontrolled low pressure (3.5–7.5 p.s.i.g.) steam oxidation of uranium	250–450	2–8	2.05–2.20	Black
Air pyrolysis of $UO_2(NO_3) \cdot 6H_2O$ to UO_3; hydrogen reduction of UO_2	480–1650	2–50	2.01–2.03	Brown
Fluidized bed denitration and UO_3 reduction	700	6	2.07	Black
Hydrogen reduction of $UO_3 \cdot 2H_2O$	850	6	2.01	Brown
Hydrogen reduction of $UO_3 \cdot H_2O$	1700	2	2.01	Gray-black
Air pyrolysis of uranium, UO_3 and UO_2 to U_3O_8; hydrogen reduction to UO_2	800	16	2.01–2.02	Brown
Hydrided-steam oxidation of uranium	150–400	12–16	2.03–2.05	Red-brown
Hydrided-air oxidized uranium; hydrogen reduction of U_3O_8 to UO_2	150–800	16	2.02	Red-brown
Direct hydrogen reduction of uranium peroxide	900	4–56	2.02–2.08	Brown
Air ignition of uranium peroxide to U_3O_8; hydrogen reduction to UO_2	900	56	2.02	Cocoa-brown
Direct hydrogen reduction of uranyl oxalate	900	64	2.01	Red-brown
Air ignition of uranyl oxalate to U_3O_8; hydrogen reduction to UO_2	900	62	2.03	Dark brown
Direct hydrogen reduction of ammonia-precipitated diuranate	900	56	2.05	Light brown
Air ignition of ammonia-precipitated diuranate to U_3O_8; hydrogen reduction to UO_2	900	80	2.13	Green-brown
Direct hydrogen reduction of ammonium hydroxide-precipitated diuranate	850–950	4–32	2.07	Brown
Air ignition of ammonium hydroxide-precipitated diuranate to U_3O_8; hydrogen reduction to UO_2	800	34	2.14	Light brown
Direct hydrogen reduction of urea-precipitated diuranate	775–800	16	2.08	Gray-brown
Air ignition of urea-precipitated diuranate to U_3O_8; hydrogen reduction to UO_2	900–1050	32	2.11	Gray-brown
Direct hydrogen reduction of ammonium carbonate-precipitated diuranate	900–1000	56–64	2.05–2.06	Dark brown
Air ignition of ammonium carbonate-precipitated diuranate to U_3O_8; hydrogen reduction to UO_2	900–1000	110–150	2.04–2.05	Brown

filtered, washed with distilled water, and dried in vacuo ($\sim 10^{-1}$ mm. of mercury) at 100° C. A series of these precipitated powders was converted into UO_2 either directly by heating in hydrogen or by first pyrolyzing the powders in air to form U_3O_8 and then reducing with hydrogen. In most cases the products were pyrophoric, oxidizing to a black material with O to U ratios ranging from 2.22 to 2.34. More stringent reduction conditions, however, gave stable brown powders.

Characterization Procedures. The UO_2 powders were analyzed for total uranium and U(IV) by titration with standard potassium dichromate (*2, 20*). The amount of U(VI) was determined polarographically (*10*). The moisture content was obtained by direct absorption in magnesium perchlorate. With these procedures, the O to U ratios of the powders were determined with an accuracy of ± 0.01 or better. Spectrographic analyses indicated that metallic impurities were less than 0.1%.

X-ray patterns were made on film using a 114.6-mm. powder camera and copper K_α radiation. The microstructure of the uranium oxide powders was examined in cross section by mounting in a plastic medium and polishing with abrasives. Viewing was done with reflected light. For the electron micrographs, the carbon replica technique was used.

Densities of the various preparations were determined by both helium and carbon tetrachloride displacement (*21, 22*). The precision of the density values obtained by helium displacement for UO_2 powders having volumes of 2 cc. was within $\pm 0.5\%$. The precision increased with increasing sample size. The UO_2 powders were degassed at a maximum pressure of 10^{-5} mm. of mercury for 1 hour at 400° C. The reproducibility of the density measurements obtained by liquid displacement was $\pm 0.2\%$.

Total surface areas were determined by volumetrically measuring the adsorption of nitrogen on UO_2 at liquid nitrogen temperature. Both the conventional BET (*7*) and the Innes (*12, 16*) methods were used. Standard techniques of degassing the UO_2 samples in vacuo at 400° C. for 1 to 4 hours and the U_3O_8 samples at 200° C. for 1 hour were adopted. Chemical analyses showed that no oxidation occurred on degassing. The uranium precipitates and UO_3 were degassed in vacuo at 80° to 100° C. for 2 hours. Values obtained on UO_2 samples treated in a similar manner agreed within $\pm 5\%$. Krypton and nitrogen adsorption measurements gave comparable results on UO_2 powders in the region of 1 square meter per gram, where both techniques were applicable (*4*).

Air permeability methods were used to give an estimate of the external surfaces of the uranium oxides. An apparatus based on the method of Gooden and Smith (*14*) was used for the coarser powders with external surfaces less than 6 square meters per cc. For the finer oxide powders, the method of Carman and Malherbe (*9*) was employed.

A commercial air sedimentation apparatus (Sharples Micromerograph, Sharples Corp., Research Laboratories, Bridgeport, Pa.) was used to obtain particle size distributions for some of the uranium oxides. A cloud of well-dispersed powder particles is introduced at the top of a pressure-tight, 220-cm., thermally insulated, sedimentation column. The particles fall because of the action of gravity, and are collected on the pan of an automatic balance which continuously records the cumulative weight collected as a function of time. These data are converted into a particle size distribution curve plotted with a template incorporating Stokes' law. For a nonspherical particle, the size measured is the diameter of a sphere which falls at the same rate.

The experimental methods have been only briefly described because these techniques and apparatus have been reported in detail (*10*).

RESULTS AND DISCUSSION

X-Ray Analyses. The crystallite size of UO_2 prepared by hydrogen reduction of UO_3 and U_3O_8 varied with temperature of reduction. UO_2 prepared at 500° C. had broader powder lines than material made at higher temperatures, indicating a smaller crystallite size. At higher reduction temperatures, the powder patterns became sharper which suggested crystallite growth. Broad powder lines were also observed for UO_2 which had been prepared by the steam oxidation of uranium. This is consistent because the steam oxidation temperatures were below 450° C. In addition U_3O_8, which was made by ignition in air at 800° C. of the UO_2 prepared by high pressure steam oxidation, yielded the sharpest U_3O_8 x-ray pattern, showing that some crystallite growth occurred during oxidation. The crystallite sizes of uranium oxide powders, thus, depend more on the temperature of preparation than on the method of preparation. This conclusion agrees with the work of Anderson (*1*).

The crystallite sizes of two representative UO_2 samples were accurately measured. The x-ray patterns for these samples were obtained on a double crystal spectrometer, and Fourier analysis of the 531 peaks was used to determine the average crystallite size. UO_2 prepared by high pressure steam oxidation of uranium at 343° C. had a crystallite size of 180 ± 20 A. Mallinckrodt PWR Core I UO_2, made by hydrogen reduction of UO_3 at 800° C., had a crystallite size of 900 ± 115 A.

Microstructure. Microscopic examination of the UO_2 powders indicated that their particle size, shape, and microstructure depended on their method of preparation. These diverse characteristics are illustrated in Figures 1 to 8. The particle sizes ranged from tenths of microns up to several millimeters. The shapes included spheres, needles, plates, and irregularly curved and angular particles. The internal particle structures varied from nearly solid chunks to very loose, spongy masses and included cluster-like and cored structures.

As shown in Figures 1 and 2, steam oxidation of uranium metal foil produced powders which were, in general, less porous in appearance than oxide prepared by reduction

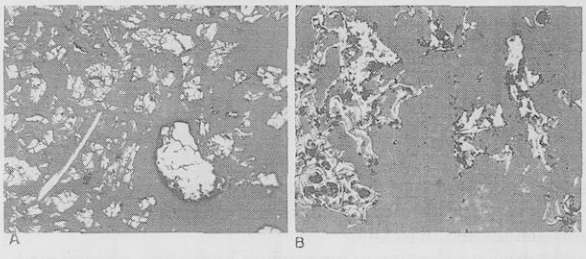

↑ Figure 1. Comparison of the two types of structure of high-pressure steam manufactured UO_2 (250×)

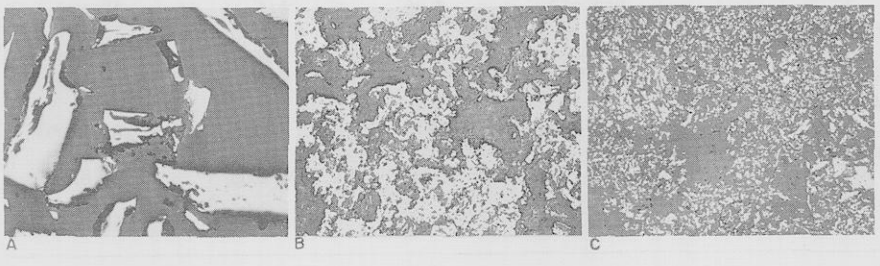

Figure 2. Microstructure comparison ← among three types of low-pressure steam manufactured UO_2 (250×)

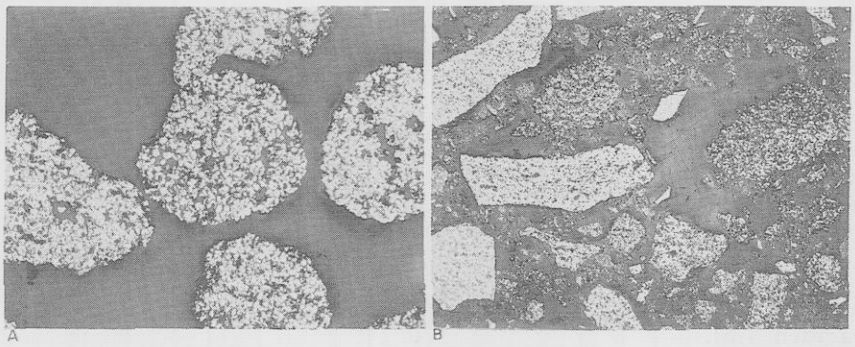

Figure 3. Two types of commercial MCW UO_2 (250×)

Figure 4. Effect of reduction temperature on microstructure of UO_2 prepared from ball-milled UO_3 (250×)

methods (Figures 3 to 8). The form of the uranium metal also has an effect on particle structure. Steam oxidation of finely divided uranium powder resulted in a finer particle structure (Figure 2,*C*) than was produced from uranium foil (Figure 2,*A*). The same effect was also found for UO_2 powders obtained by hydrogen reduction of U_3O_8 prepared from uranium powder and foil.

The UO_2 powders prepared by the high pressure steam oxidation method were of two types: One contained thin, sheet-like particles (Figure 1,*B*); the other was composed of more massive and angular particles having numerous cracks (Figure 1,*A*). The cause of this difference in particle structure is not known. The low pressure steam oxidation method also resulted in two particle types. In this case, however, the difference can be attributed to reaction conditions. The UO_2 prepared by controlled oxidation contained needles and plates having sharp edges (Figure 2,*A*) and its gross appearance is consistent with its very low surface area. The oxide powder made by uncontrolled oxidation was spongy in appearance (Figure 2,*B*) and had a higher surface area.

Mallinckrodt PWR Core I UO_2, made by reduction of UO_3, was composed of roughly spherical porous particles with a cluster-like structure. Figure 3,*A*, shows its general shape and porous structure. Little variation was found in general structure with sieve size, which is consistent with surface area and density measurements. The distinctly different microstructure of the Mallinckrodt oxide prepared from ammonium diuranate is shown in Figure 3,*B*. The particles reveal a variety of irregular shapes and sizes.

UO_2 prepared by hydrogen reduction of ball-milled UO_3 was similar in structure to the Mallinckrodt PWR Core I powder, but its particle size was somewhat finer, which is in agreement with its higher surface area (Figure 4,*B*). The particle size showed a marked dependence on temperature of reduction. Surface area and density measurements as well as the microstructure (Figure 4) indicate a considerable increase in particle size with increase in reduction temperature. A similar effect was observed for UO_2 preparations made by reduction of both UO_3 and U_3O_8. The higher the reduction temperature, the coarser was the particle structure.

UO_2 particles prepared by the spray denitration technique were rounded and had a cored particle structure (Figure 5,*A*). Their microstructure shows some indication of accessible internal porosity, which would explain their relatively high density and surface area. UO_2 particles obtained by reduction of the hydrothermally grown $UO_3 \cdot H_2O$ crystals were large-grained rhombohedra (Figure 5,*B*) which showed a considerable amount of closed porosity consistent with their low density and surface area. The parent UO_3 particle shape was retained essentially in both of these processes.

Microscopic examination of ammonium diuranate crystals produced by addition of ammonium hydroxide to uranyl nitrate solution, showed a wide range of irregular shapes and sizes (1 to 600 microns). Ammonium diuranate crystals obtained from the urea reaction varied in size, but

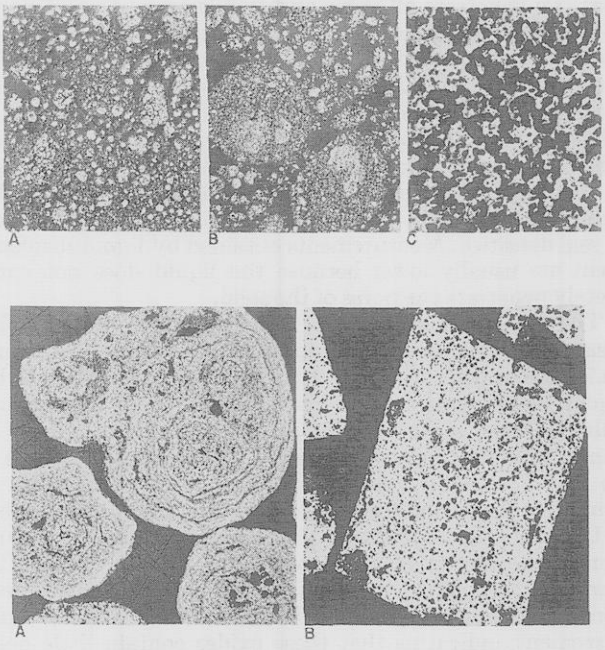

Figure 5. Microstructure of UO_2 powders prepared by reduction of higher uranium oxides (250×)

were more uniform (roughly spherical) in shape. Precipitation from ammonium carbonate medium yielded uniform, spherical particles. Very fine, minute diuranate particles were obtained with gaseous ammonia. These differences in crystal appearance may be attributed to the mechanism of precipitation. Ammonium hydroxide gives an immediate precipitate even when added dropwise, whereas the slow decomposition of urea results in slow homogeneous generation of ammonium hydroxide from within the solution. Ammonium carbonate first causes the precipitation of ammonium uranyl carbonate, which is then decomposed by boiling to form ammonium diuranate.

A comparison of photomicrographs of the uranium oxides obtained from these diuranate powders shows similar differences in crystal appearance. UO_2 prepared from ammonium hydroxide-precipitated diuranate varied in size and shape. Urea-precipitated diuranate yielded oxide with somewhat less particle structure variation. However, U_3O_8 and UO_2 made from ammonium diuranate precipitated with ammonium carbonate were composed of fairly uniform spheres (Figure 6). In these preparations, the microstructure of the original ammonium diuranate is retained on conversion to U_3O_8 and UO_2. However, the microstructure of the uranium oxide powders prepared from ammonia-precipitated diuranate, uranyl oxalate, and uranium peroxide was distinctly different from that of the starting uranium precipitates. The U_3O_8 and UO_2 obtained from diuranate precipitated with gaseous ammonia were massive and angular in appearance (Figure 7), while the oxides made from oxalate were acicular (Figure 8). The fact that the U_3O_8, the U_3O_8-reduced UO_2,

and the precipitate-reduced uranium dioxide have almost identical microstructures can be used as evidence of a reduction mechanism for the uranium precipitates in which they are first converted into U_3O_8 which is subsequently reduced to UO_2.

Density Measurements. The theoretical densities of UO_2, U_3O_8, and UO_3 are 10.96, 8.39, and 8.34 grams per cc. (*18*). This "ideal," crystallite, or x-ray density is calculated from the size of the unit cell and the atomic weights of the constituents, assuming that all lattice points are occupied. However, experimental density values for the uranium oxides vary over a wide range, depending on the experimental technique and the method of preparation (*18*). Density data, obtained from the displacement of a fluid that can penetrate all pores and capillaries of a solid down to molecular dimensions, are termed "real" densities. Closed pores, which are voids, completely surrounded by the solid, are arbitrarily considered as part of the real volume of the material. The helium atom has a small molecular diameter which enables it to penetrate into very fine pores. In addition, there is negligible adsorption of helium on solids at room temperature (*6*). Therefore, densities obtained by helium displacement most closely conform to the definition of real densities. Measurements obtained by liquid displacement are usually lower because the liquid does not completely penetrate the pores of the solid.

The measured densities of UO_2 powders, prepared by steam oxidation procedures, approach the theoretical value, 10.96 grams per cc. (Table II). The densities obtained by liquid displacement are slightly lower than the helium values. Thus, it is likely that these powders consist of dense granules (no closed porosity) with varying amounts—up to 3% of total volume—of small open pores. This is confirmed by the microscopic studies previously mentioned.

Density values for the UO_2 powders prepared by reduction of the higher uranium oxides are given in Table III. For the most part, the helium and liquid displacement densities are considerably below theoretical and in close agreement, indicating that these oxides contain little open porosity, but an appreciable amount of closed porosity. Only in the case of powders prepared by the fluidized processes are the liquid values lower, suggesting the presence of small, open pores. When high density UO_2 prepared by the high pressure steam oxidation method was ignited to U_3O_8 and converted back to UO_2 by reduction, the real density (10.69 grams per cc.) of the product was still higher than the densities (10.02 to 10.35 grams per cc.) of the other U_3O_8-reduced UO_2 powders.

In addition, as shown in Table IV, the lower the density

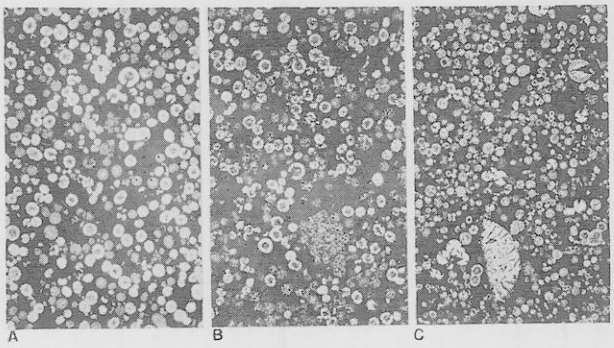

Figure 6. UO_2 prepared from $(NH_4)_2CO_3$-precipitated diuranate (250×)

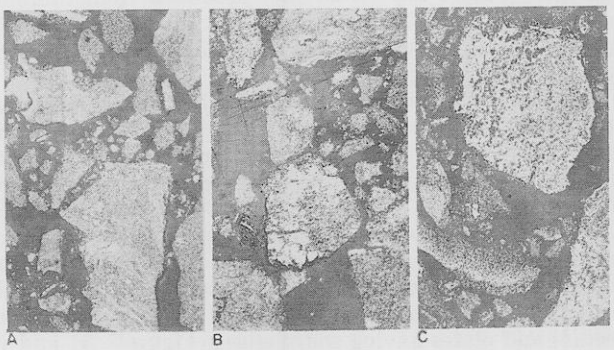

Figure 7. UO_2 prepared from NH_3-precipitated diuranate (250×)

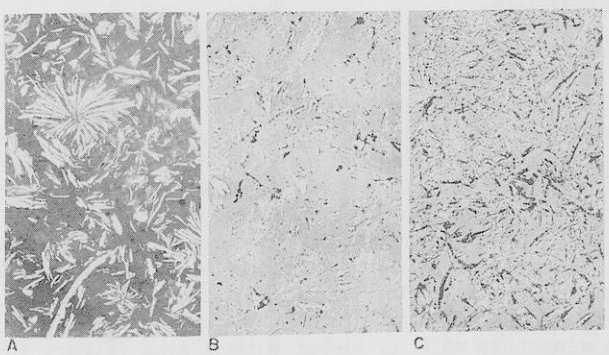

Figure 8. UO_2 prepared from uranyl oxalate (250×)

Table II. Properties of UO_2 Prepared by Steam Oxidation Methods

Method of Preparation	Reaction Conditions	O/U	Density, G./Cc. He	Density, G./Cc. CCl_4	Density, G./Cc. Bulk	Surface Area, Sq. M./Cc BET, Sg.	Permeability Porosity	Permeability Sp.	Roughness Factor, Sg/Sp
High pressure steam oxidation of uranium	72-Hr. oxidation at 343° C. and 2200 p.s.i.g.	1.97	10.92 ± 0.1	10.75	2.76	12.9	0.645	3.1	4.2
Controlled low pressure steam oxidation of uranium	24-Hr. oxidation at 150° C. and 5 p.s.i.g.; dried 8 hr. in vacuo at 700° C.	2.02	10.85 ± 0.1	10.91	1.75	2.4	0.645	3.2	0.8
Uncontrolled low pressure steam oxidation of uranium	5-Hr. oxidation at 350° C. and 5 p.s.i.g.; heated in hydrogen 5 hr. at 900° C.	2.03	10.92 ± 0.05	10.85	2.47	9.0	0.645	2.7	3.3
Steam oxidation of uranium from uranium hydride	4-Hr. oxidation at 400° C. and 5 p.s.i.g.; heated in hydrogen 15 hr. at 700° C.	2.03	10.98 ± 0.1	10.67	1.75	22.6	0.686	5.6	4.0

Table III. Properties of UO_2 Prepared by Reduction of the Higher Uranium Oxides

Method of Preparation	Reaction Conditions	O/U	Density, G./Cc. He	Density, G./Cc. CCl_4	Density, G./Cc. Bulk	Surface Area, Sq. M./Cc. BET, Sg	Surface Area, Sq. M./Cc. Permeability Porosity	Surface Area, Sq. M./Cc. Permeability Sp	Roughness Factor, Sg/Sp
Hydrogen reduction of $UO_3 \cdot 2H_2O$	6 Hr. at 850° C.	2.01	10.25 ± 0.05	10.25	2.12	8.8	0.645	4.1	2.2
Hydrogen reduction of $UO_3 \cdot H_2O$ crystals grown hydrothermally in an autoclave	2 Hr. at 1700° C.	2.01	10.34 ± 0.05	10.37	4.63	0.5	0.455	0.6	0.8
Hydrogen reduction of UO_3 made by denitration in a fluidized bed	16 hr. at 800° C.	2.02	10.13 ± 0.10	9.94	3.85	9.5	0.645	2.8	3.4
Fluidized bed denitration and UO_3 reduction	6 Hr. at 700° C.	2.07	10.54 ± 0.05	10.28	4.19	30.6	0.645	2.3	13.3
MCW PWR Core I UO_2: cracked ammonia reduction of UO_3	4 Hr. at 815° C.	2.02	10.16 ± 0.05	10.13	2.77	6.4	0.645	3.1	2.1
Air ignition of MCW UO_2 to U_3O_8; hydrogen reduction to UO_2	24-Hr. oxidation at 800° C.; 15-hr. reduction at 780° C.	2.01	10.35 ± 0.10	10.32	2.21	5.4	0.645	3.3	1.6
Air ignition of high pressure steam oxidized UO_2 to U_3O_8; hydrogen reduction to UO_2	24-Hr. oxidation at 800° C.; 15-hr. reduction at 780° C.	2.01	10.69 ± 0.10	10.67	1.82	4.3	0.645	3.2	1.3
Air pyrolysis of $UO_2(NO_3) \cdot 6H_2O$ to U_3O_8; hydrogen reduction to UO_2	48-Hr. oxidation at 740° C.; 16-hr. reduction at 800° C.	2.02	10.03 ± 0.05	9.96	1.98	5.7	0.645	3.3	1.7
Air pyrolysis of $UO_2(NO_3) \cdot 6H_2O$ to U_3O_8; hydrogen reduction to UO_2	15-Hr. oxidation at 800° C.; 16-hr. reduction at 800° C.	2.01	10.02 ± 0.10	10.07	1.93	5.8	0.645	3.0	1.9
Hydrided-air oxidized uranium; hydrogen reduction of U_3O_8 to UO_2	24-Hr. oxidation at 740° C.; 16-hr. reduction at 800° C.	2.02	10.32 ± 0.15	10.46	1.10	9.4	0.739	5.4	1.7

Table IV. Comparison between Surface Area and Density of UO_2 Powders and Their Parent Compounds

Compound	Method of Preparation	Helium or Liquid Fluid Density, G./Cc. Compound	Helium or Liquid Fluid Density, G./Cc. UO_2	Total Surface Area, Sq. M./Cc. Compound	Total Surface Area, Sq. M./Cc. UO_2
$UO_2(NO_3)_2 \cdot 6H_2O$	Evaporation of uranyl nitrate solution	2.75	...	2.4	...
UO_3	Pyrolysis of $UO_2(NO_3)_2 \cdot 6H_2O$	7.32	10.16	9.1	6.4
UO_3	Pyrolysis of $UO_2(NO_3)_2 \cdot 6H_2O$; milled	7.66	10.36	21.2	13.8
$UO_3 \cdot H_2O$	Grown hydrothermally in an autoclave	5.84	10.34	1.1	0.5
$(NH_4)_2U_2O_7$	NH_4OH precipitation from uranyl nitrate solution	4.96	11.11	72.4	37.4
U_3O_8	Air ignition of NH_4OH-precipitated diuranate at 500° C.	7.50	11.09	73.2	59.9
U_3O_8	Air ignition of NH_4OH-precipitated diuranate at 800° C.	8.10	10.61	8.8	9.7
$(NH_4)_2U_2O_7$	Urea precipitation from uranyl nitrate solution	5.62	10.74	31.3	42.1
U_3O_8	Air ignition of urea-precipitated diuranate at 500° C.	7.53	11.34	74.3	60.4
U_3O_8	Air ignition of urea-precipitated diuranate at 800° C.	8.15	10.55	5.1	6.0
$(NH_4)_2U_2O_7$	$(NH_4)_2CO_3$ precipitation from uranyl nitrate solution	5.75	10.30	31.0	40.7
U_3O_8	Air ignition of $(NH_4)_2CO_3$-precipitated diuranate at 500° C.	7.32	10.30	41.0	36.2
U_3O_8	Air ignition of $(NH_4)_2CO_3$-precipitated diuranate at 1000° C.	7.94	10.46	8.6	14.1
$(NH_4)_2U_2O_7$	NH_3 precipitation from uranyl nitrate solution	4.82	10.85	93.6	40.8
U_3O_8	Air ignition of NH_3-precipitated diuranate at 500° C.	8.00	10.46	102.7	58.0
$UO_4 \cdot 2H_2O$	H_2O_2 precipitation from uranyl nitrate solution	3.99	10.38	11.0	12.0
U_3O_8	Air ignition of uranium peroxide at 500° C.	7.09	10.44	15.7	11.9
$UO_2(C_2O_4) \cdot H_2O$	Oxalic acid precipitation from uranyl nitrate solution	3.73	10.61	2.9	7.3
U_3O_8	Air ignition of uranyl oxalate at 500° C.	8.22	10.68	66.0	30.4

of a UO_3 preparation, the lower the density of the resulting UO_2. The persistence of low density during the oxidation and reduction of MCW PWR Core I UO_2 emphasizes this point. The dependence of the density of a UO_2 preparation upon the density of the substance from which it has been made by reduction is in agreement with the work of Anderson and others (*1*).

The density measurements for UO_2 powders prepared by direct reduction of the uranium precipitates are listed in Table V. In general, the helium displacement density values of the UO_2 powders prepared from ammonium diuranate and uranium peroxide were close to the theoretical value of 10.96 grams per cc. The liquid displacement densities were below the helium values, suggesting that these powders have varying amounts of small, open pores. Densities obtained by both helium and liquid displacement for the UO_2 preparation made from uranyl oxalate were below theoretical and identical, indicating that this oxide contains no open porosity, but a measurable amount of closed porosity.

As seen in Table IV, there seems to be no apparent

Table V. Properties of UO_2 Prepared By Direct Reduction of Uranium Precipitates

Source	Reduction Conditions	O/U	Density, G./Cc.			Surface Area, Sq. M./Cc.			Roughness Factor, Sg/Sp
			He	CCl_4	Bulk	Sg	Permeability Porosity	Permeability Sp	
Ammonium hydroxide–precipitated diuranate	32 hr. at 850°–950° C.	2.07	11.11 ± 0.2	10.81	1.07	37.4	0.771	13.9	2.7
Urea precipitated–diuranate	16 Hr. at 800° C.	2.08	10.74 ± 0.2	10.19	0.83	42.1	0.750	12.6	3.3
Ammonia precipitated–diuranate	56 Hr. at 900° C.	2.05	...	10.85	1.79	40.8	0.590	3.5	11.7
Ammonium carbonate–precipitated diuranate	64 Hr. at 900° C.	2.06	...	10.30	1.50	40.7	0.765	4.1	9.9
Uranium peroxide	4 Hr. at 900° C.	2.08	11.00 ± 0.1	10.78	1.34	28.4	0.651	9.8	2.9
Uranyl oxalate	64 Hr. at 900° C.	2.01	10.61 ± 0.2	10.61	1.07	7.3	0.780	5.0	1.5

Table VI. Properties of UO_2 Prepared by Reduction of U_3O_8 Obtained from Uranium Precipitates

Method of Preparation	Reduction Conditions	O/U	Density, G./Cc.			Surface Area, Sq. M./Cc.			Roughness Factor, Sg/Sp
			He	CCl_4	Bulk	BET, Sg	Permeability Porosity	Permeability Sp	
MCW UO_2: pyrohydrolysis of ammonium hydroxide–precipitated diurante; reduction to UO_2	Reduced with cracked ammonia	2.02	10.75 ± 0.1	10.84	2.07	15.4	0.660	3.3	4.7
Air ignition (500° C.) of ammonium hydroxide–precipitated duranate; hydrogen reduction to UO_2	34 Hr. at 800° C.	2.14	11.09 ± 0.15	10.77	1.38	59.9	0.731	12.9	4.6
Air ignition (800° C.) of ammonium hydroxide–precipitated diuranate; hydrogen reduction to UO_2	25 Hr. at 900° C.	2.02	10.61 ± 0.15	10.71	0.89	9.7	0.656	5.5	1.8
Air ignition (500° C.) of urea-precipitated diuranate; hydrogen reduction to UO_2	32 Hr. at 900°–1050° C.	2.11	11.34 ± 0.2	10.47	1.00	60.4	0.768	10.3	5.9
Air ignition (800° C.) of urea-precipitated diuranate; hydrogen reduction to UO_2	40 Hr. at 900° C.	2.01	10.55 ± 0.15	10.43	1.41	6.0	0.727	3.7	1.6
Air ignition (500° C.) of ammonia precipitated diurante; hydrogen reduction to UO_2	80 Hr. at 900° C.	2.13	10.75 ± 0.15	10.82	1.50	58.0	0.654	16.8	3.4
Air ignition (500° C.) of ammonia-precipitated diuranate; hydrogen reduction to UO_2	110 Hr. at 900° C.	2.05	...	10.30	1.61	36.2	0.766	3.9	9.3
Air ignition (1000° C.) of ammonium carbonate–precipitated diuranate; hydrogen reduction to UO_2	16 Hr. at 900° C.	2.02	...	10.46	1.77	14.1	0.706	3.1	4.5
Air ignition (500° C.) of uranium peroxide; hydrogen reduction to UO_2	56 Hr. at 900° C.	2.02	...	10.44	1.91	11.9	0.650	3.2	3.7
Air ignition (500° C.) of uranyl oxalate; hydrogen reduction to UO_2	62 Hr. at 900° C.	2.03	...	10.68	0.98	30.4	0.788	6.6	4.6

relationship between the densities of the uranium precipitates and the densities of the resulting UO_2 powders. Thus, ammonium diuranate powders with densities of 4.82 and 5.75 grams per cc. yielded $UO_{2.06}$ with densities of 10.85 and 10.30 grams per cc., respectively.

Densities for the UO_2 powders prepared by reduction of U_3O_8 obtained from the uranium precipitated (Table VI) vary over a wide range. For Mallinckrodt oxide, the helium and carbon tetrachloride densities are high and in close agreement, indicating little porosity. Powders for which the helium and liquid displacement density values are below theoretical and in close agreement, contain little open porosity, but some closed porosity. For several of the UO_2 powders, the liquid displacement densities were less than the helium values, indicating the presence of open porosity.

The data of Table IV, which indicate that the density of these UO_2 powder depends upon the density of the U_3O_8 from which they have been prepared by reduction, are consistent with the results of Anderson and others (*1*). Two apparent exceptions, where low density U_3O_8 (7.50 and 7.53 grams per cc.) yielded very high density UO_2 (11.09 and 11.43 grams per cc., respectively), can be partially explained as caused by the high O to U ratios (2.14 and 2.11, respectively) of these UO_2 powders. Using kerosine as a displacing liquid, Gronvold (*15*) found that the density of his UO_2 preparations increased from 10.79 to 11.16 as the O to U ratio increased from 2.00 to 2.25. In a recent study (*11*) using helium and carbon tetrachloride as displacing media, it was found that uranium oxide samples with O to U ratios from 2.10 to 2.24, had measured densities which

varied from 10.13 to 10.42. The density of a UO_2 preparation, therefore, depends upon its O to U ratio as well as on the density of its parent higher oxide.

Surface Area Measurements. Surface area measurements obtained by gas adsorption techniques measure the total area of a solid. Permeability methods measure only the surface of a solid available to flow, while the adsorption method measures total accessible surface. Surface areas attributed to surface roughness and internal surface porosity are not measured (*8*). However, the ratio of the surface areas determined by the gas adsorption and permeability methods, termed the "roughness factor," may give some indication of the degree of porosity, irregularity, and nonuniformity of the powder particles. When this ratio is unity, a powder can be considered as nonporous. Thus, the relationship between gas adsorption and permeability measurements of surface area is similar to that between measurements of density by helium and liquid displacement.

The total (BET) and external (permeability) surface areas for UO_2 powders prepared by steam oxidation procedures are listed in Table II. The surface areas are reported per unit volume of solid material, rather than per unit mass in order to compare areas of powders with different densities. For the most part these UO_2 powders had relatively low total surface areas, which is reasonable, because the UO_2 preparations were made from uranium metal foil which itself has a low surface area. Because a fine powder is made by the decomposition of UH_3, UO_2 prepared by steam oxidation of hydrided uranium had a much greater surface area than the oxides made by other steam oxidation methods. The total and external specific surface areas for the UO_2 prepared by the controlled, low pressure, steam oxidation technique were approximately equal. This is in agreement with photomicrograph and density data which show that this oxide powder is composed of coarse, dense particles with no open porosity. For the other powders, the external surface areas were lower than the total surface areas, which is again consistent with microscopic and density results in showing coarse, dense particles with varying amounts of open porosity.

As shown in Table III, hydrogen reduction of the higher uranium oxides usually resulted in UO_2 powders with relatively low total surface areas and roughness factors. The total surface areas and roughness factors of UO_2 prepared by both fluidized bed denitration and UO_3 reduction were much higher than those of oxide made by fluidized bed denitration and standard hydrogen reduction of UO_3. This, in agreement with microscopic and density data, indicates that the former powder is more porous and contains many more surface irregularities which gas molecules can penetrate. Surface areas and roughness factors of UO_2 powders prepared by hydrogen reduction of U_3O_8 were very low. Only U_3O_8 made by ignition of finely powdered uranium from UH_3 gave a UO_2 powder with a higher specific surface area than the Mallinckrodt oxide, and even then the value was less than half that of UO_2 prepared by steam oxidation of the same uranium powder. As discussed later, the 800° C. temperature of preparation of the U_3O_8 may have contributed to the low specific surfaces. The roughness factors (1.3 to 2.0) of these powders are consistent with their helium and liquid displacement densities in showing the presence of little or no open porosity.

In agreement with the results of other workers (*1, 5, 19*) the data of Table IV and Figure 9 show that the total surface areas of the UO_2 preparations made from UO_3 depend on the surface area of the UO_3 rather than on that of the original uranyl nitrate hexahydrate, and on the temperature of reduction. UO_3 powders with surface areas of 2.76 and 1.24 square meters per gram yielded, under approximately the same reduction conditions (16 hours and 800° C.), UO_2 preparations with surface areas of 1.33 and 0.63 square meter per gram, respectively. The extremely low

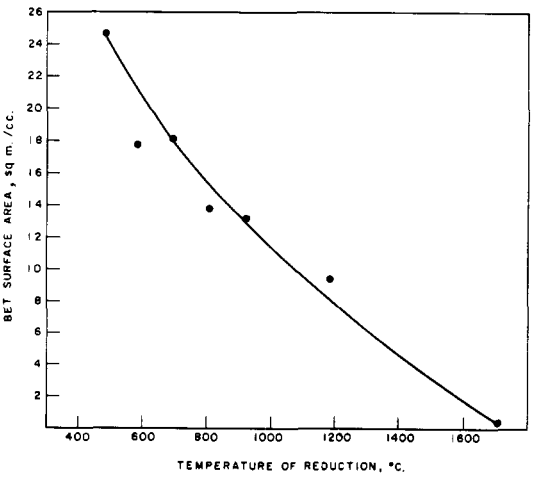

Figure 9. Surface area as a function of reduction temperature

total surface (0.05 square meter per gram) of UO_2 prepared by the crystal growth method is probably caused by both the low surface area of the parent $UO_3 \cdot H_2O$ (0.19 square meter per gram) and the high temperature of reduction, 1700° C.

The marked dependence of total surface area on temperature of reduction is shown in Figure 9. Only at a reduction temperature of 480° C. was the surface area of the UO_2 (2.37 square meters per gram) equivalent to that of the parent UO_3 (2.76 square meters per gram). In agreement with microscopic observations (Figure 4), both total surface and roughness factor decreased as the reduction temperature increased, indicating a considerable amount of particle growth and decrease of porosity. Below 1650° C., the temperature of reduction did not seem to affect either the fluid or bulk density values. Those preparations with slightly greater densities had somewhat higher O to U ratios. At 1650° C., however, there was a noticeable increase in both fluid and bulk densities and the roughness factor decreased to approximately unity. Most of the closed pores were eliminated, and large-grained, nonporous UO_2 particles resulted. Anderson and others (*1*) also observed that heating low density UO_2 caused an increase in its density.

Total surface area and fluid density measurements were performed on ammonium diuranate, uranium peroxide, uranyl oxalate, and U_3O_8 powders in an effort to ascertain any correlation between the properties of the precipitate, the intermediate U_3O_8, and the resulting UO_2. The results are given in Table IV. Ammonium diuranate prepared by precipitation with gaseous ammonia and ammonium hydroxide had the largest specific area, the lowest density, and on the basis of x-ray measurements, the smallest crystallite size. This is consistent with the fact that precipitation with these reagents occurs rapidly and forms a finely divided, poorly crystallized powder. Precipitation from urea and ammonium carbonate solution occurs slowly and yields a material of larger crystallite and particle size and smaller specific surface.

Although both of these diuranate powders were prepared by methods involving slow precipitation, microscopic examination showed that the ammonium carbonate-precipitated diuranate was composed of uniform, spherical particles, whereas the diuranate particles obtained from urea solution were somewhat distributed in size and shape. This suggests that the former is a more carefully crystallized powder and contains fewer closed pores, a conclusion which is borne out by its greater density. The similarity in surface area may indicate that its average particle size is smaller than that of the urea-precipitated diuranate.

Surface area measurements for UO_2 powders prepared by

direct reduction of the uranium precipitates are given in Table V. The total surface areas and roughness factors were usually somewhat lower than those of UO_2 powders prepared by first pyrolyzing the precipitates to U_3O_8 at 500° C. and then reducing with hydrogen (Table VI). The high roughness factors (10 to 12) for UO_2 powders prepared from ammonium carbonate and ammonia-precipitated diuranate are consistent with their microscopic appearance, which shows extremely porous particles. The low roughness factor (1.5) for UO_2 obtained from uranyl oxalate agrees with the liquid and helium displacement density values in showing no open porosity. The electron micrographs showed in Figure 10 support these conclusions. A roughness factor

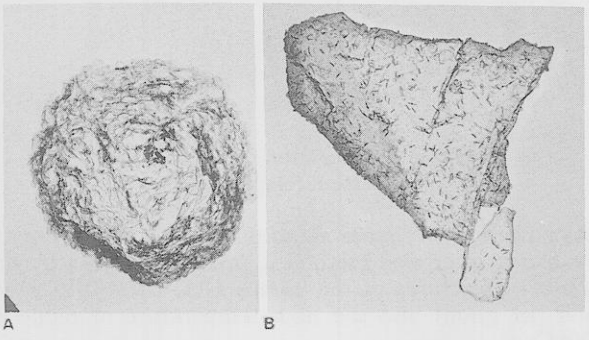

Figure 10. Electron micrographs of UO_2 powders prepared by precipitation procedures (9000×)

of approximately 3 was found for the remainder of these UO_2 preparations, which was consistent with density measurements in indicating the presence of some open pores. As seen in Table IV, there is no apparent relationship between the specific surface area of the parent ammonium diuranates and the derivative UO_2 powders. Although, the urea- and ammonium carbonate–precipitated diuranates had approximately 40% of the area of the diuranates obtained by ammonia addition, the final UO_2 powders had almost equal surface areas.

Surface area values for UO_2 powders prepared by reduction of U_3O_8 obtained from uranium precipitates are listed in Table VI. Total surface areas for these powders were the highest of all UO_2 preparations surface areas studied, although the temperatures of reduction were 900° C. or higher in most cases. However, UO_2 powders obtained by reduction of U_3O_8, prepared by air ignition at 800° to 1000° C., had low total and external surface areas. The U_3O_8 ignition temperatures, therefore, are important in determining U_3O_8 and UO_2 product surface areas. The data of Table IV, again in agreement with the results of other workers (*1, 5*), clearly show the dependence of the surface areas of these UO_2 preparations upon the surface areas of the parent U_3O_8. As was found for the other UO_2 preparations, the roughness factors (4.5 to 6) in Table VI correlated generally with density measurements, in indicating varying amounts of open porosity. A high roughness factor (9.3) was again found for UO_2 prepared from ammonium carbonate–precipitated diuranate.

Surface area measurements performed on UO_2 powders that had been reduced from U_3O_8 at 700°, 600°, and 500° C. gave values for the specific surface of 0.37, 0.40, and 0.65 square meter per gram, respectively, as compared with a value of 0.33 square meter per gram for the original U_3O_8 powder. An increasing amount of breakdown, therefore, occurs as the temperature of reduction is lowered (*1, 3, 13*). Greater particle breakdown probably occurs at the lower temperatures because mobility is lower in solids, and strains resulting from phase transformation are less easily annealed out at lower temperatures. The breakdown itself can be explained on the basis of the difference in crystal structure and density, an orthorhombic unit cell of density 8.39 grams per cc. changing to a cubic cell of density 10.96 grams per cc. No particle breakdown was observed when β-cubic U_4O_9 (0.46 and 0.73 square meter per gram) and hexagonal UO_3 (2.77 square meters per gram) samples were reduced at 410° and 480° C. to UO_2 (0.45, 0.80, and 2.37 square meters per gram), respectively.

Particle Size Distribution Analyses. Surface area and average particle diameters can also be calculated by sedimentation and elutriation techniques which are used basically for measuring particle size distributions. One might expect reasonable agreement between surface areas and average particle diameters calculated from permeability measurements and from particle size distribution measurements, because in both cases the geometric sizes of the particles are of primary importance. However, as shown in the following paragraphs, average particle diameters calculated from particle size distribution measurements are generally severalfold greater than those calculated from permeability measurements. The difference can be attributed to the fact that most powders are agglomerated—i.e., they are composed of aggregates of more or less loosely bound discrete particles. However, the three experimental techniques together give much complementary information on the size, shape, degree of porosity, and degree of aggregation of powder particles.

The particle size distribution curves (determined by air sedimentation) for several representative UO_2 powders are plotted in Figure 11. All the powders have a wide range of particle size, varying generally from 5 to 50 microns. Although an "average" particle diameter of about 2 microns is obtained from permeability measurements for these UO_2

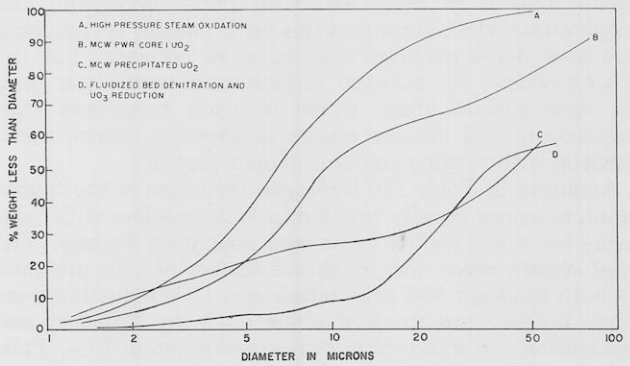

Figure 11. UO_2 particle size distribution
Effect of powder preparation

powders, their particle size distributions differ appreciably. The large particle size of the UO_2 prepared by spray denitration and fluidized bed reduction is consistent with microscopic, density, and roughness factor data in indicating that this powder is composed of highly porous particles.

The effect of the ammonium diuranate precipitant on the particle size distribution of UO_2 powders is given in Figure 12. Particle size analyses are in agreement with microscopic evidence. The UO_2 particles prepared from ammonium hydroxide and ammonia-precipitated diuranate varied widely in size; urea-precipitated diuranate yielded oxide with less particle size variation, whereas UO_2 made from ammonium diuranate precipitated with ammonium carbonate had a relatively narrow size range.

The size distributions of Mallinckrodt uranyl nitrate hexahydrate, UO_3 and UO_2, show that the particle size range of Mallinckrodt UO_2 is much closer to that of the parent UO_3 than to that of the starting uranyl nitrate hexahydrate. This indicates, as with surface area and density, that particle size distribution of a UO_2 preparation

is dependent (disregarding reduction temperature variation) upon that of the higher parent oxide. In agreement with microscopic and surface area measurements, a considerable amount of particle growth was observed as the reduction temperature increased. Only at a reduction temperature of 480° C. was the particle size distribution of UO_2 similar to that of the parent UO_3.

Studies were made of the effect of oxidation or reduction on particle size distribution and total surface area of uranium oxides. A decrease occurred in both particle size and BET surface area when Mallinckrodt PWR Core I UO_2 and ammonium carbonate-precipitated diuranate were oxidized to U_3O_8 at 800° and 1000° C. Thus, while some sintering occurred at these temperatures to give a lower total surface area, the oxidation process tends to break up the agglomerates. No change in particle size distribution, but an increase in surface area, was observed on low temperature reduction (500° C.) of U_3O_8 to UO_2. Particle breakdown occurred and gave an increased total surface area, but the integrity of the agglomerates was retained. Finally, there was no change in either particle size distribution or surface area on low temperature reduction (410° C.) of U_4O_9 to UO_2. In this case, neither particle nor agglomerate breakdown occurred. This appears reasonable, because there are no large changes in either crystal structure or density with the reduction of U_4O_9 to UO_2.

SUMMARY

The results of the studies of Anderson and others (*1*) concerning the dependence of UO_2 properties upon their mode of preparation are confirmed and their conclusions extended to UO_2 powders made by a large variety of oxidation and reduction methods. Although physical properties such as particle size and distribution, microstructure, porosity, crystallite size, surface area, and density can vary over a wide range, these properties can be controlled through the judicious choice of variables in the preparation procedure.

To a first approximation, the crystallite size of UO_2 powders depends more on the temperature than on the method of preparation. Low temperature preparations (350° C.) produced the smallest crystallite sizes (200 A.); the crystallite size of UO_2 made at 800° C. was considerably larger (1000 A.).

The real density of a UO_2 preparation depends upon its O to U ratio and on the density of its parent higher oxide. The density was not dependent on reduction temperature up to 1200° C. However, heating low density UO_2 above its temperature of preparation can cause an increase in its density. In many cases the liquid displacement densities were considerably below the helium displacement values, indicating measurable amounts of open porosity.

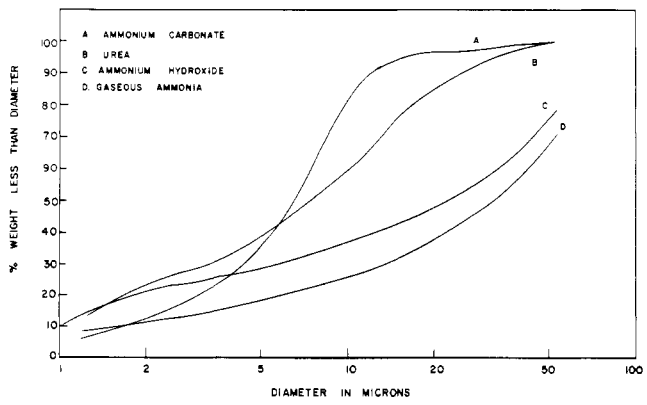

Figure 12. UO_2 particle size distribution
Effect of precipitation

There is no correlation between density and total BET surface area; a high surface area can be associated with either a high or a low density; a low surface area powder can have either a low or a high density. There appears to be no relationship between the density and total surface area of the parent ammonium diuranate precipitates and the derivative UO_2 powders.

The particle size distribution and total BET surface area of a UO_2 preparation depend upon the particle size distribution and surface area of the higher oxide from which it has been prepared by reduction and on the reduction temperature itself. In the reduction of UO_3, the uranium dioxide reduction product was most similar in surface area and particle size distribution to the parent oxide at low temperatures (480° C.). Particle growth occurred at higher temperatures. No change in particle size distribution, but an increase in surface area was observed on low temperature reduction (500° C.) of U_3O_8 to UO_2. There was less particle breakdown at higher reduction temperatures. This suggests that fracturing occurs in the U_3O_8 particles on reduction to UO_2 at the lower temperature; at higher temperatures, the strains are annealed out.

ACKNOWLEDGMENT

The authors thank Jack Belle for his interest and helpful criticism, Z.M. Shapiro for initiating this study, R.B. Roof for crystallite size measurements, T.R. Padden for advice in interpretation of microscopic data, and R.T. Parks, J.E. Rulli, P.S. Schnizler, F.C. Schrag, and K.R. Bauer for assistance with the experimental work.

LITERATURE CITED

(1) Anderson, J.S., Harper, E.A., Moorblath, S., Roberts, L.E.J., At. Energy Research Establ. (Gt. Brit.) **C/R 886** (1952).
(2) Anonson, S.H., U. S. At. Energy Comm. **MDDC-1435** (1947).
(3) Bard, R.J., U. S. At. Energy Comm. **LA 1952** (1955).
(4) Beebe, R.A., Beckwith, J.B., Honig, J.M., *J. Am. Chem. Soc.* **67**, 1554 (1945).
(5) Bel, A., Carteret, Y., Proc. 2nd. U. N. Intern. Conf. Peaceful Uses At. Energy, Geneva, **6**, 612 (1958).
(6) Brunauer, S., "Adsorption of Gases and Vapors," pp. 380–5, Princeton University Press, 1943.
(7) Brunauer, S., Emmett, P.H., Teller, E., *J. Am. Chem. Soc.* **60**, 309 (1938).
(8) Carman, R.C., "Flow of Gases through Porous Media," Chap. VI, Academic Press, New York, 1956.
(9) Carman, R.C., Malherbe, P. le R., *J. Soc. Chem. Ind.* **69**, 134 (1950).
(10) Clayton, J.C., Aronson, S., U. S. At. Energy Comm. **WAPD-178** (1958).
(11) Clayton, J.C., Aronson, S., *Bettis Tech. Rev.* **10**, 96 (1958).
(12) Clayton, J.C., Rulli, J.E., *Chemist-Analyst* **47**, 62 (1958).
(13) De Hollander, W.R., U. S. At. Energy Comm. **HW-46685** (1956).
(14) Gooden, E.L., Smith, C.M., *Ind. Eng. Chem., Anal. Ed.* **12**, 479 (1940).
(15) Gronvald, F., *J. Inorg. & Nuclear Chem.* **1**, 357 (1955).
(16) Innes, W.B., *Anal. Chem.* **23**, 759 (1951).
(17) Johnson, J.R., Fulkerson, S.D., Taylor, A.J., *Bull. Am. Ceram. Soc.* **36**, 112 (1957).
(18) Katz, J.J., Rabinowitch, E., "The Chemistry of Uranium," McGraw-Hill, New York, 1951.
(19) Lister, B.A.J., Gillies, G.M., "Process Chemistry," p. 19, McGraw-Hill, New York, 1956.
(20) Rodden, C.J., "Analytical Chemistry of the Manhattan Project," McGraw-Hill, New York, 1950.
(21) Rossman, R.P., Smith, W.R., *Ind. Eng. Chem.* **35**, 972 (1943).
(22) Smith, R.C., Jr., Howard, H.C., *Ibid.*, **34**, 438 (1942).
(23) Stenquist, D.R., Mastel, B., Anicetti, R.J., *J. Am. Ceram. Soc.* **41**, 273 (1958).

RECEIVED for review October 7, 1959. Accepted June 20, 1960.

Division of Industrial and Engineering Chemistry, 133rd Meeting, ACS, San Francisco, Calif., April 1958.